

RESEARCH

Open Access



A study of cadmium yellow paints from Joan Miró's paintings and studio materials preserved at the Fundació Miró Mallorca

Mar Gomez Lobon^{1*}, Marta Ghirardello^{2*}, Enric Juncosa Darder³, Carlos Palomino Cabello⁴, Marta Bauza⁴, Marine Cotte^{5,6}, Aviva Burnstock⁷, Austin Nevin⁷, Silvia Rita Amato⁷, Francesca Caterina Izzo⁸ and Daniela Comelli²

Abstract

The deterioration of cadmium yellow paints in artworks by Joan Miró (1893–1983) and in painting materials from his studios in Mallorca (Spain) was investigated. Analysis of samples from Miró's paintings and from paint tubes and palettes showed that degraded paints are composed of poorly crystalline cadmium sulfide/zinc cadmium sulfide ($CdS/Cd_{1-x}Zn_xS$) with a low percentage of zinc, in an oil binding medium. Cadmium sulfates were identified as the main deterioration products, forming superficial white crusts detected using SR μ XANES and μ XRD techniques. Time-resolved photoluminescence measurements demonstrated that highly degraded samples display a pink/orange emission from the paint surface with a microsecond lifetime, a phenomenon observed in other degraded cadmium yellow paints. In agreement with recent studies on altered cadmium paints, these results suggest that the stability of the paint is related to its manufacturing method, which affects the degree of crystallinity of the resulting pigment. This, together with the environmental conditions in which artworks have been exposed, have induced the degradation of yellow paints in Miró's artworks. It was finally noted that the paints exhibiting alteration in the analysed Miró artworks have a chemical composition that is very similar to the tube paint 'Cadmium Yellow Lemon No. 1' produced by *Lucien Lefebvre-Foinet*. Indeed, paint tubes from this brand were found in the studio, linking the use of this product with Miro's degraded artworks.

Keywords Joan Miró, Artist's studio, Cadmium yellow, Pigment deterioration, Twentieth-century painting materials

[†]Mar Gomez Lobon and Marta Ghirardello share first co-authorship.

*Correspondence:

Mar Gomez Lobon
info@artco-services.com

Marta Ghirardello
marta.ghirardello@polimi.it

¹ Artco Services, Mallorca, Spain

² Physics Department, Politecnico di Milano, Milan, Italy

³ Conservation Department, Fundació Pilar i Joan Miró a Mallorca, Palma de Mallorca, Spain

⁴ Chemistry Department, Universitat de les Illes Balears, Palma de Mallorca, Spain

⁵ European Synchrotron Radiation Facility (ESRF), Grenoble, France

⁶ Laboratoire d'Archéologie Moléculaire et Structural (LAMS) CNRS UMR 8220, Sorbonne Université, Paris, France

⁷ Conservation Department, The Courtauld Institute of Art, London, UK

⁸ Heritage and Conservation Science, Department of Environmental Sciences, Informatics and Statistics, Ca' Foscari University of Venice, Venice, Italy



© The Author(s) 2023. **Open Access** This article is licensed under a Creative Commons Attribution 4.0 International License, which permits use, sharing, adaptation, distribution and reproduction in any medium or format, as long as you give appropriate credit to the original author(s) and the source, provide a link to the Creative Commons licence, and indicate if changes were made. The images or other third party material in this article are included in the article's Creative Commons licence, unless indicated otherwise in a credit line to the material. If material is not included in the article's Creative Commons licence and your intended use is not permitted by statutory regulation or exceeds the permitted use, you will need to obtain permission directly from the copyright holder. To view a copy of this licence, visit <http://creativecommons.org/licenses/by/4.0/>. The Creative Commons Public Domain Dedication waiver (<http://creativecommons.org/publicdomain/zero/1.0/>) applies to the data made available in this article, unless otherwise stated in a credit line to the data.

Introduction

Joan Miró (Barcelona 1893–Palma de Mallorca 1983) is one of the great artists of the twentieth century. The originality of Miró's works in art forms ranging from painting, paper and sculpture to monumental ceramic murals, painted textiles and even theatre set designs, strongly influenced the artistic practice of the twentieth century. Miró's most prolific and experimental production was in Mallorca, from 1956 until his death in 1983. For the first time, he had extensive studio spaces (known as *Taller Sert* and *Son Boter*) that allowed him to work on large-format artworks, and on many works simultaneously. The Mallorca studios have been preserved as the artist left them at his death, including over a hundred tubes of oil paints, cans of synthetic paints, palettes, and other materials. These offer rich resources for the study of Miró's painting materials and techniques. The investigation of the materials left in the artist's studios, complemented with the study of micro-samples taken from his artworks, provide useful information for understanding Miró's materials. It also helps to comprehend changes they have undergone after ageing, which may also contribute to the interpretation and conservation of the artworks. Other studies of artists' studio materials have shown the importance of these kinds of collections [1–5].

The Fundació Miró Mallorca, built around Miró's studios, also holds an extensive archive and a large collection of artworks that were left there after Miró's death [6]. By examining the artist's works, conservators at the Fundació noted that some passages of yellow paint have discoloured and, in some cases, have become powdery, resulting in significant visual changes. As an example, *Femme dans la rue* (1973) appears in a 1978 photograph with Miró in his *Taller Sert* studio (Fig. 1a). When

compared to its current condition, the original vibrant yellow appears to have faded (Fig. 1b). A total of 26 artworks in the collection present these phenomena, all painted in the 1970s. This deterioration is also observed in the paints on some of the artist's palettes preserved in the studios.

During this study, the degraded paints were identified as cadmium yellow (CdY), a colour favoured by Miró throughout his career. In a letter written to his friend Enric Ricart during his formative years, Miró wrote: "Instead of chrome, I recommend ... cadmium lemon, it is splendid... Chrome, next to cadmium lemon, is a dull and lightless colour." [7]. CdY has been characterised in two of his works from the 1930s [8, 9] and all the orange and yellow paints found in his studios in Mallorca are cadmium-based [10].

Cadmium yellow is a synthetic pigment based on cadmium sulfide (CdS), which began to be commercialised for artistic purposes from 1840 [11]. Lighter CdY paints, usually containing zinc, correspond to a later date of pigment production (from 1920) [11]. Cadmium yellow was quickly adopted by many artists including Van Gogh, Picasso, Seurat, Matisse and Munch [11]. It appears that cadmium sulfide produced in the late nineteenth and early twentieth centuries was poorly lightfast, resulting in discolouration in many works of art after only 20 years [11]. The deterioration of CdY-based paints has been reported in paintings including *The Scream* by Edvard Munch [12, 13], as well as in other artworks by Van Gogh [14, 15], Matisse [16–19], James Ensor [20] and Picasso [21, 22]. Through these studies and further analyses on model paints, the degradation pathway of CdY—from the yellow cadmium sulfide (CdS) to the white cadmium sulfates ($\text{CdSO}_4/\text{CdSO}_4 \cdot \text{H}_2\text{O}$)—was

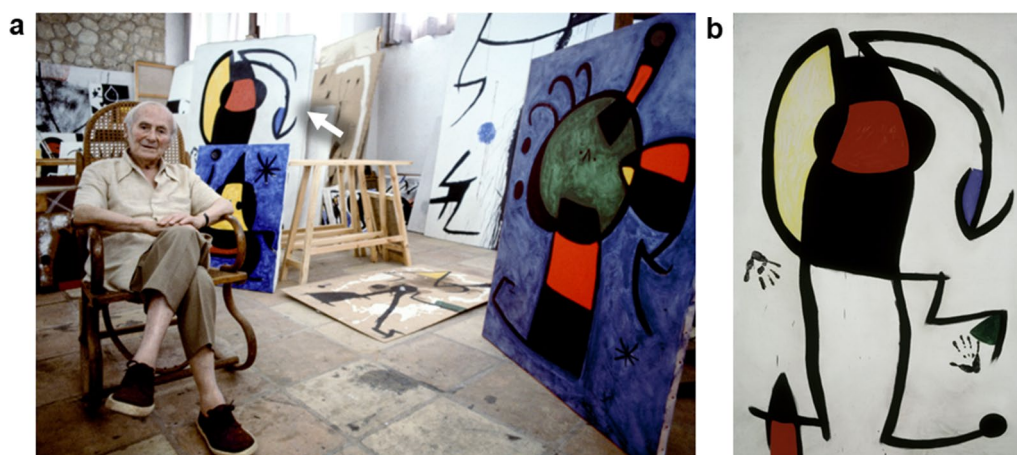


Fig. 1 Photograph of Joan Miró in his studio *Taller Sert* in 1978 (© Jean Marie del Moral) (a), showing the original condition of *Femme dans la rue* (1973) (b), now showing discolouration of the original vibrant yellow

established, and the possible factors that have a key role in CdS paints degradation were identified [23]. Studies on model paints have demonstrated that the degradation of CdY is triggered by light and/or high relative humidity ($\geq 95\%$) and that zinc cadmium sulfide ($\text{Cd}_{1-x}\text{Zn}_x\text{S}$) solid solutions are more susceptible to photo-oxidation than pure CdS. Moreover, residues of the synthesis (e.g., chlorine/chloride species [13, 18]) and early imperfect synthesis processes [15, 19, 24] may play a role in CdS paint stability. Most of the reported studies are related to paintings dating from the late nineteenth and early twentieth centuries, while the artworks by Miró were painted in the 1970s. Therefore, the collection of Fundació Miró Mallorca represents a unique case study for examining the deterioration of this paint at a later stage of pigment production history [11].

In this work, nine samples of yellow paint from both artworks and studio materials were analysed. The aims of this study are to (i) identify the composition of the yellow paints and understand the characteristics of the CdS pigment present therein, (ii) compare the composition of artist studio materials with the artworks, and (iii) propose factors that could have triggered the degradation of the CdY paints.

Materials and methods

Samples selection and preparation

Under visible light, most of the 26 artworks in the collection that present CdY deterioration show loss of the intensity of the yellow colour, as well as chalking: a form of deterioration where the paint becomes crumbly and

powdery. In some artworks, a whitish crust was observed on the superficial paint layer—hiding a more intense yellow layer underneath—and some small shiny crystal-like efflorescence was visible with the naked eye. In other paintings, where the paint layer was thinly applied, the yellow had become nearly transparent (see Additional file 1: Fig. S1).

Paint microsamples were taken from three representative artworks from the collection of the Fundació Miró Mallorca, which show deterioration of the yellow oil paint (see Fig. 2). Microsamples of yellow paint were also collected from three paint tubes from different brands (*Lucien Lefebvre-Foinet*, *Mir* and an unknown one), a cup used for mixing paint, and two palettes (Additional file 1: Fig. S2). These paint tubes and objects were found in *Taller Sert* and *Son Boter* studios. Table 1 presents the full description of the samples and their provenance.

All artworks had been displayed in the artist's studio *Taller Sert* from the time they were painted in the 1970s until they were moved to the new museum building, completed in 1992, and later replaced with replicas. It is worth noting that the studio *Taller Sert* has an uncontrolled environment with intense natural light through window glass. Recent datalogger readings show temperatures reaching over 30 °C in the summer and levels of relative humidity (RH) over 80% in the winter. The artworks in the studio were exposed to these conditions for around two decades.

The paint tubes and the palettes were kept in the studios *Taller Sert* and *Son Boter* until the time of the

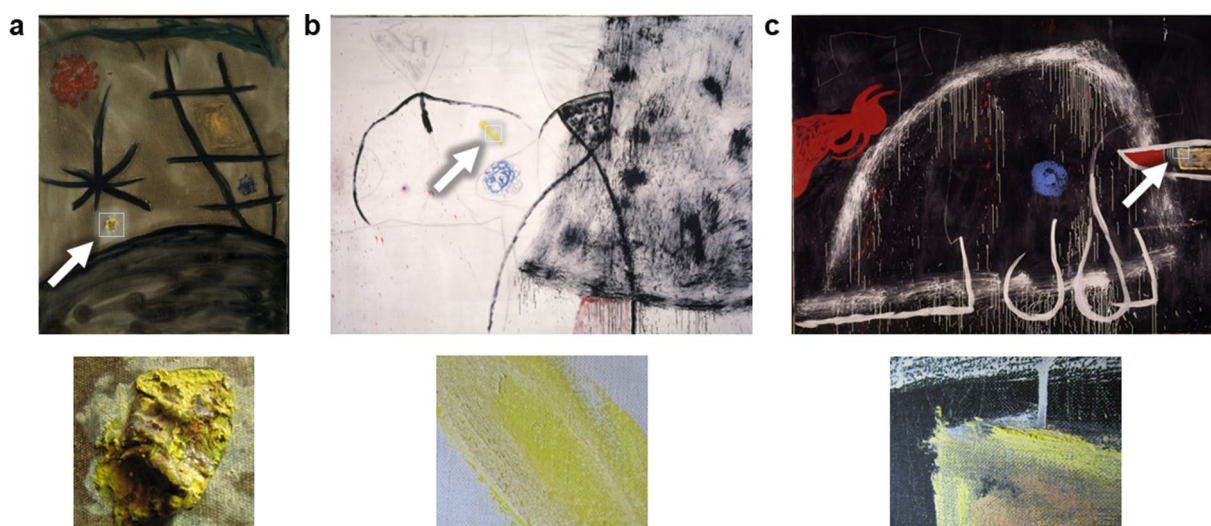
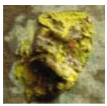


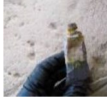


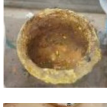




Fig. 2 Sampled artworks by Joan Miró and macro images of the sampled yellows (marked with white dotted rectangles and arrows in the artworks). **a** *Untitled* (FPJM-00029), 1978, oil on canvas, 92 × 72.5 cm (sample A2). **b** *Untitled* (FPJM-00054.1), 1973, Oil, acrylic and charcoal on canvas, 270 × 355 cm (sample A7). **c** *Untitled* (FPJM-00053), 1974, Oil, acrylic and chalk on canvas, 270.5 × 355 cm (sample A9)

Table 1 Samples name, image of the object or of the point on the artwork from which the sample was taken, description of the sampled artwork/object and of the region where the samples were taken

Sample name	Artwork/object image	Description of the sampled artwork/object	Sampled region	
Artworks	A2		Untitled-FPJM-00029 Oil on canvas 1978	Visibly degraded yellow paint, discoloured and chalky. Sample taken from a thick area of impasto
	A7		Untitled-FPJM-00054.1 Oil, acrylic and charcoal on canvas 1973	Visibly degraded yellow paint, discoloured and powdery, with some whitish crusts on the surface
	A9		Untitled-FPJM-00053 Oil, acrylic and chalk on canvas 1974	Visibly degraded yellow paint, discoloured and powdery, with some whitish crusts on the surface
Oil paint tubes	A3		Tube of yellow oil paint <i>Mir</i> Artist studio <i>Son Boter</i>	Yellow sample taken from the dry paint around the edge of the paint tube
	A5		Tube of Cadmium Yellow Lemon No.1 <i>Lucien Lefebvre-Foinet</i> Artist studio <i>Son Boter</i>	Yellow sample taken from the inside of the paint tube (liquid)
	A6		Tube of yellow oil paint Unknown brand, possibly <i>Mir</i> Artist studio <i>Taller Sert</i>	Yellow sample taken from the dry paint around the edge of the paint tube
Artist palettes	A1		Cup used for mixing paint Artist studio <i>Taller Sert</i>	Visibly degraded yellow paint, discoloured and chalky
	A4		Artist palette Artist studio <i>Taller Sert</i> ^a	Yellow sample taken from the edge of the yellow paint on the palette
	A12		Artist palette Artist studio <i>Taller Sert</i>	Visibly degraded yellow paint, discoloured and chalky. Sample taken from the edge of the yellow paint on the palette

^a Inside a display case from 1986 to 2018, then removed and placed in the *Taller Sert* studio

analyses except for one of the palettes (from which sample A4 was taken). This palette was donated by the Miró family to the Fundació in 1986 and was displayed inside an enclosed case (made of glass and with a wooden board covered with fabric inside) until 2018, when it was removed from the display case and placed in the *Taller Sert*.

When the amount of the collected material was sufficient, part of it was analysed without embedding it in resin. In the other cases, where the available material was limited, samples were prepared as cross-sections embedded in epoxy resin (ResinPro[®]) followed by dry hand polishing with abrasive sheets (Micro-Mesh[®]).

Multi-analytical approach

Samples were analysed using a multi-analytical approach that included investigation using elemental, structural, molecular and luminescence techniques, as described below.

Scanning electron microscopy with energy dispersive X-ray analysis (SEM-EDX)

Elemental analyses were performed on raw samples A1–A6 with a scanning electron microscope (SEM, Hitachi S-3400N, used at 15 kV), equipped with a Bruker AXS XFlash 4010 EDS system. Elemental mapping of cross-sections of samples A7, A9, A12 was performed using a

Zeiss EVO LS15 SEM–EDX used at 20 kV. The samples were carbon-coated prior to EDX mapping to improve surface conductivity.

X-ray diffraction (XRD)

Identification of crystalline phases was performed using X-ray diffraction analysis on unmounted samples (A1–A6) using a Bruker D8 Advance diffractometer with monochromatised CuK_α radiation (1.54 Å) at 40 kV and 40 mA.

Synchrotron Radiation (SR) μXRD mapping on micro cross-sections (samples A4, A7, A9 and A12) and paint tube fragment (sample A5) was performed at the ID13 beamline of the European Synchrotron Radiation Facility (ESRF, Grenoble), benefitting from the Historical Materials BAG [25]. The μXRD branch was used to perform crystalline phase mapping using a $2.5 \times 2.5 \mu\text{m}^2$ beam with an energy of 13 keV. Two-dimensional (2D) diffraction patterns were collected in transmission mode at every pixel of 2D maps and converted into 1D diffractograms by azimuthal integration, using the Jupyter Notebooks based on the PyFAI software package [26].

In both cases, the identification of the crystalline phases was performed using Match! and QualX software, while maps analysis was carried out with PyMca software [27].

Micro X-ray fluorescence (μXRF) and X-ray absorption near edge structure (μXANES)

High lateral resolution information on the distribution and speciation of S of samples A7, A9, A5, A4 and A12 was obtained by performing hyperspectral 2D μXRF mapping and μXANES spectroscopy analysis in XRF mode at S K-edge at the scanning X-ray microscope end-station hosted at the beamline ID21 of the ESRF (Grenoble, France) [28, 29]. The energy calibration was performed using reference powders of $\text{CaSO}_4 \cdot 2\text{H}_2\text{O}$. The incident beam was focused with Kirkpatrick-Baez mirrors down to a beam of $0.5 \times 0.6 \mu\text{m}^2$ ($h \times v$). Hyperspectral 2D μXRF maps were recorded by scanning the energy across the S K-edge employing the following conditions: from 2.46 to 2.4675 keV, 2.5 eV step; from 2.468 to 2.485 keV, 0.5 eV step; from 2.49 to 2.53 keV, 2 eV step. An additional map employing a monochromatic primary beam of fixed energy at 3.573 keV was acquired, to excite Cd at its L_3 -edge. The software PyMca was used to fit the XRF spectra and to separate the contribution of different elements. S^{-II} and S^{VI} chemical state maps are obtained by extracting the maps obtained at the energy of 2.473 keV and 2.482 keV to favour the excitation of the S^{-II} and S^{VI} species respectively and following the procedure described in literature [20]. XANES spectra from

selected regions of interests (ROIs) of hyperspectral 2D μXRF maps were also extracted and compared.

Fourier-transformed infrared spectroscopy (FTIR)

FTIR analyses were performed on unmounted samples A1–A6 in transmission mode with a Bruker Tensor 27 system in the spectral range 4000 cm^{-1} to 400 cm^{-1} , with 3 cm^{-1} of resolution and accumulating 32 scans.

Micro Attenuated Total Reflectance ($\mu\text{-ATR}$) FTIR was carried out on points of the cross-sections using a Thermo Nicolet iN10 MX spectrometer equipped with an MCT/A detector cooled with liquid Nitrogen and a Germanium crystal, with a real aperture of $25 \times 25 \mu\text{m}^2$. Data were collected in the range $4000\text{--}750 \text{ cm}^{-1}$, at a spectral resolution of 4 cm^{-1} and with 256 average scans. Spectra are displayed without correction for ATR.

Micro photoluminescence (μPL) measurements

The PL properties of the microsamples were probed with a time-gated photoluminescence microscopy system, fully described elsewhere [30]. The system is based on a pulsed Q-switching laser source ($\lambda_{\text{em}} = 355 \text{ nm}$, pulse duration = 1 ns, repetition rate = 100 Hz, FTSS 355–50, Crylas GmbH) and time-gated detector (C9546-03, Hamamatsu Photonics and R6, Qimaging). The image detector is coupled to an epi-fluorescence microscope equipped with a $50\times$ ($\text{NA} = 0.5$) refractive objective, providing imaging from a circular field of view $300 \mu\text{m}$ in diameter with a spatial resolution of $0.6 \mu\text{m}$. By using a time-gated approach and coupling the detection with a hyperspectral system, it is possible to reconstruct time-gated hyperspectral images of the PL emission at different timescales.

Raman spectroscopy

Raman spectra were acquired using an inVia Qontor confocal Raman microscope (Renishaw plc, Wotton-under-Edge, UK). The spectra were recorded using the 785 nm laser excitation, a 1200 lines/mm dispersive grating, and $50\times$ long-distance magnification with 1 cm^{-1} spectral resolution and $1 \mu\text{m}$ spatial resolution. The spectra were acquired using the WiRE 5.5 software. The acquisitions varied between 5 and 20 s, 2 to 118 mW power, 5 and 20 accumulations.

Py/GC–MS and GC–MS

According to a procedure described in [2, 31–33], Py/GC–MS analysis was conducted on micro fragments of the samples (approximately $0.30 \mu\text{g}$) for a preliminary screening regarding organic composition. After ascertaining the presence of lipid-bound paint, it was decided

Table 2 Results of the multi-analytical characterisation performed on the samples

Sample name	Elemental composition		Molecular composition				Photoluminescence properties			
	SEM-EDX	SR μ XRF	SR μ XRD	SR μ XANES	FTIR	GC-MS	Raman	Time-gated μ PL microscopy		
Artworks	A2	Cd, S (Zn)	NA	NA	Oil (2916, 2847, 1714 cm^{-1}) Carboxylates (1537 cm^{-1}) Sulfates (1096, 606 cm^{-1}) Oxalates (1615, 1319 cm^{-1})	Drying oil, likely linseed oil (P/S = 1.87), relatively dried (A/P = 1.21, O/S = 0.40)	CdS/Cd _{1-x} Zn _x S (238, 305, 346 cm^{-1}) Oil (869 cm^{-1}) 3CdSO ₄ ·8H ₂ O (476, 983, 1006 cm^{-1}) Unassigned: 411 cm^{-1}	Homogeneous μ s emission along the paint stratigraphy, broad and weak, peaked at 700 nm (DTS CdS/Cd _{1-x} Zn _x S)		
Artworks	A7	Cd, S (Zn)	Cd, S (Zn)	NA	Poorly crystalline CdS/Cd _{1-x} Zn _x S (bulk) 3CdSO ₄ ·8H ₂ O (surface)	Sulfide (bulk) Sulfates (surface)	Oil (2925, 2850, 1706 cm^{-1}) Carboxylates (1560 cm^{-1}) Sulfates (1087 cm^{-1})	Drying oil, likely linseed oil (P/S = 1.78) as stand oil (typical markers of pre-polymerisation treatments), relatively dried (A/P = 1.17, O/S = 0.15)	CdS/Cd _{1-x} Zn _x S (218, 238, 305, 346 and 633 cm^{-1}) Oil (869 cm^{-1}) 3CdSO ₄ ·8H ₂ O (476, 983 and 1006 cm^{-1}) Unassigned: 411 cm^{-1}	Spatially heterogeneous emission, with the paint surface displaying a broad and intense μ s emission peaked at 695 nm (DTS CdS/Cd _{1-x} Zn _x S), very weak emission from the bulk
Artworks	A9	Cd, S (Al, Si)	Cd, S	NA	Poorly crystalline CdS/Cd _{1-x} Zn _x S (bulk) 3CdSO ₄ ·8H ₂ O (surface)	Sulfide (bulk) Sulfates (surface)	No FTIR spectra due to strong resin background	Drying oil, likely safflower oil (P/S = 2.20), very dried (A/P = 1.45, O/S = 0.02)	CdS/Cd _{1-x} Zn _x S (238, 305, 633 cm^{-1}) 3CdSO ₄ ·8H ₂ O (476, 983 and 1006 cm^{-1}) Unassigned: 411 cm^{-1}	Spatially heterogeneous emission, with the paint surface displaying a broad and intense μ s emission peaked at 690 nm (DTS CdS/Cd _{1-x} Zn _x S), very weak emission from the bulk

Table 2 (continued)

Sample name	Elemental composition		Crystalline phases		Molecular composition				Photoluminescence properties	
	SEM-EDX	SR μ XRF	XRD	SR μ XRD	SR μ XANES	FTIR	GC-MS	Raman	Time-gated μ PL microscopy	
Oil paint tubes A3	Cd, S (Mg, Al)	NA	Crystalline hexagonal CdS	NA	NA	Oil (2917, 2850, 1705 cm^{-1}) Carboxylates (1563 cm^{-1}) Mg-carbonate (1455, 1415, 873, 822 cm^{-1}) Mg-sulfate (1080, 983 cm^{-1})	Drying oil, likely linseed oil (P/S = 1.35), not very well dried; traces of beeswax and alkyl-based resin; high amount of unsaturated oleic and linoleic acids	No Raman bands detectable due to strong fluorescence	Homogeneous emission in the paint layer, with a sharp and strong ns peak at 517 nm (NBE CdS) and a broad μ s peak above 800 nm (DTS CdS)	
A5	Cd, S (Zn)	NA	Poorly crystalline CdS/Cd _{1-x} Zn _x S	Poorly crystalline CdS/Cd _{1-x} Zn _x S	Mainly sulfide, low quantities of sulfates	Oil (2924, 2853, 1738 cm^{-1}) Carboxylates (1550 cm^{-1}) Sulfates (1100, 610 cm^{-1})	Drying oil, likely safflower/sunflower oil (P/S = 2.89), not very dried; traces of a <i>Pinaceae</i> resin (i.e., Colophony); high amount of unsaturated oleic and linoleic acids	CdS/Cd _{1-x} Zn _x S (218, 238, 305, 346 and 633 cm^{-1}) Oil (869, 1063, 1080, 1304, 1441, 1657, 1740, 2853, and 2909 cm^{-1}) 3CdSO ₄ ·8H ₂ O (983 and 1006 cm^{-1}) Unassigned: 411 cm^{-1}	Homogeneous emission with a weak ns sharp peak at 485 nm (NBE Cd _{1-x} Zn _x S) and a broad μ s emission peaked above 750 nm (DTS Cd _{1-x} Zn _x S)	
A6	Cd, S (Mg, Al)	NA	Crystalline hexagonal CdS	NA	NA	Oil (2920, 2850, 1701 cm^{-1}) Mg-carbonate (3393, 1456, 1407, 826 cm^{-1}) Mg-sulfate (1073, 983, cm^{-1}) Oxalates (1606, 1320 cm^{-1})	Drying oil, likely linseed oil (P/S = 1), very well dried; metal soaps	No Raman bands detectable due to strong fluorescence	Homogeneous emission, sharp at 515 nm (NBE CdS), broad μ s emission peak above 800 nm (DTS CdS)	

Table 2 (continued)

Sample name	Elemental composition		Crystalline phases			Molecular composition				Photoluminescence properties	
	SEM-EDX	SR μ XRF	XRD	SR μ XRD	SR μ XANES	FTIR	GC-MS	Raman	Time-gated μ PL microscopy		
Artist palettes A1	Cd, S (Zn)	NA	Poorly crystalline CdS/Cd _{1-x} Zn _x S	NA	NA	Oil (2916, 2847, 1710 cm ⁻¹) Carboxylates (1537 cm ⁻¹) Sulfates (1082, 606 cm ⁻¹) Oxalates (1621, 1319, 822 cm ⁻¹)	Drying oil, likely linseed oil (P/S = 1.75), dried; traces of a Pinacaeae resin (i.e., Colophony)	No Raman bands detectable due to strong fluorescence	Spatially heterogeneous emission, with the paint surface displaying a broad and intense μ s emission peaked at 655 nm (DTS CdS/Cd _{1-x} Zn _x S), weak emission from the bulk		
A4	Cd, S (Zn)	Cd, S (Zn)	Poorly crystalline CdS/Cd _{1-x} Zn _x S	Poorly crystalline CdS/Cd _{1-x} Zn _x S	Sulfide (bulk) Sulfates (concentrated in Zn rich region detected in the μ XRF mapping)	Oil (2917, 2849, 1733 cm ⁻¹) Carboxylates (1540 cm ⁻¹) Sulfates (1100, 606 cm ⁻¹)	Drying oil, likely linseed oil (P/S = 1.30), dried; traces of a Pinacaeae resin (i.e., Colophony)	CdS/Cd _{1-x} Zn _x S (238, 305, 346, and 633 cm ⁻¹) Oil (869, 1063, and 1080 cm ⁻¹) 3CdSO ₄ ·8H ₂ O (476, 983 and 1006 cm ⁻¹) Unassigned: 411 cm ⁻¹	Homogeneous μ s emission at 700 nm (DTS CdS/Cd _{1-x} Zn _x S)		
A12	Cd, S (Zn, Cl)	Cd, S (Zn)	NA	Poorly crystalline CdS/Cd _{1-x} Zn _x S (bulk) 3CdSO ₄ ·8H ₂ O (surface)	Sulfide (bulk) Sulfates (surface)	Oil (2923, 2850, 1710 cm ⁻¹) Carboxylates (1540 cm ⁻¹) Sulfates (1097, 1043 cm ⁻¹) Oxalates (1612, 1317, 827 cm ⁻¹)	Drying oil, likely linseed oil (P/S = 1.45), dried; traces of a Pinacaeae resin (i.e., Colophony)	No Raman bands detectable due to strong fluorescence	Spatially heterogeneous emission, with the paint surface displaying a broad and intense μ s emission peaked at 650 nm (DTS CdS/Cd _{1-x} Zn _x S), weak emission from the bulk		

to perform a quantitative analysis of the paint samples via GC–MS to establish the exact nature of the identified lipid fraction and to obtain the molar ratios of the most significant fatty acids found within the samples. The procedure used is detailed in the literature [34–37] and has already been successfully applied on modern and contemporary oil paintings. The molar ratios among the most important fatty acids considered are: Azelaic to Palmitic (A/P), Oleic to Stearic (O/S) and Palmitic to Stearic (P/S).

Results

Results of samples characterisation are summarised in Table 2.

Elemental composition and crystalline phases

Elemental analyses revealed that the samples from artworks, palettes and *Lucien Lefebvre-Foinet* paint tube (sample A5) are similar in elemental composition, containing as main elements: Cd, S and a low quantity of Zn (Additional file 1: Figs. S3 and S4). In samples A3 and A6, only Cd and S were detected, together with small peaks for Mg, Al and Si. These elements may be indicative of the presence of additives such as kaolin and magnesium carbonate (as confirmed by FTIR analysis). Al and Si traces were also found in sample A9, while sample A12 presents small traces of Cl.

X-ray diffraction analyses showed that samples from all of the artworks, palettes and paint tube A5 are composed of poorly crystalline CdS or $\text{Cd}_{1-x}\text{Zn}_x\text{S}$ in mixed crystalline form (hexagonal and cubic). Due to the broad diffraction peaks (Fig. 3), it was not possible to establish the amount of Zn present by estimating the shift of the diffraction peaks with respect to the reference CdS pattern [38]. Instead, paint tubes A3 and A6 show the presence of crystalline hexagonal CdS (Fig. 3b). Moreover, most of

the samples from artworks or palettes analysed through SR μXRD (A7, A9, A12), show the presence of cadmium sulfate hydrate ($3\text{CdSO}_4 \cdot 8\text{H}_2\text{O}$) at the paint surface or within the paint layer (Additional file 1: Fig. S5), related to paint degradation.

Molecular composition

FTIR spectra from the paint fragments and cross-sections (Additional file 1: Fig. S6) show the typical peaks associated with fatty acids at ca. 2920, 2850 [$\nu(\text{CH})$], and 1710–1730 [$\nu(\text{CO})$] cm^{-1} , suggesting a lipid-containing binding medium [39]. In most of the samples, IR bands at 1560–1530 cm^{-1} were also detected, ascribed to the presence of metal carboxylates (Cd and Zn ones [40, 41]), formed as a consequence of the reaction of free fatty acids with metal cations or intentionally added to the paint tube formulation as additives [42, 43]. Magnesium carbonate (ca 1450, 1415, 875, 820 cm^{-1}) was also detected in *Mir* paint tubes (samples A3 and A6). This compound was used in the formulation of twentieth century oil paints tubes as an additive [42–45].

Cadmium sulfate in hydrated form was detected in all the samples from artworks and palettes. The sulfate was particularly evident in all the samples from artworks (broad band in 1000–1100 cm^{-1} range and below 650 cm^{-1}) and from palettes A1 and A12. Interestingly, sulfates were also found in samples from the *Lucien Lefebvre-Foinet* paint tube (sample A5). Cd and/or Zn oxalates were also found in samples A1 and A2, through the absorption bands at ca 1620, 1320 and 820 cm^{-1} . These compounds can form due to the reaction between Zn^{2+} and Cd^{2+} ions of the pigment and oxalate ions resulting from the oxidation of the oil binder [46, 47].

The presence of cadmium sulfate hydrate was also confirmed using Raman spectroscopy (Additional file 1: Fig. S7), which detected the bands at 476, 983 and 1006 cm^{-1} ,

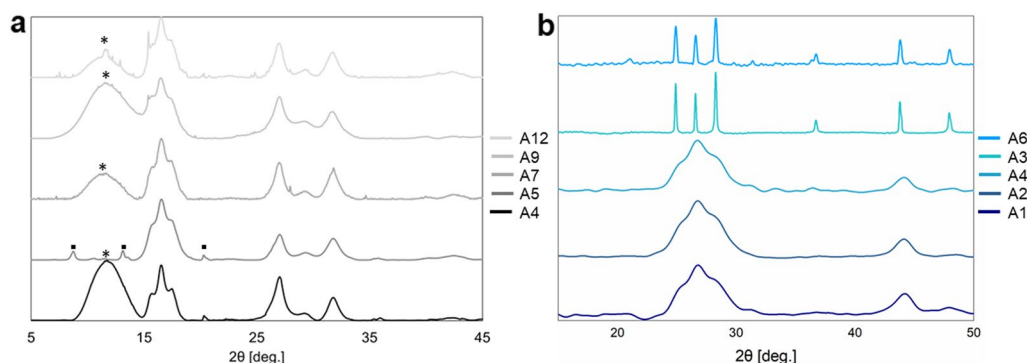


Fig. 3 **a** SR μXRD patterns of samples A4, A5, A7, A9 and A12 recorded at beamline ID13 of ESRF employing a beam with an energy of 13 keV. The broad peak between 8 and 14°, indicated with an asterisk, is related to the embedding resin, while other sharp peaks in samples A7, A9 and A12 can be ascribed to cadmium sulfate hydrate. Peaks indicated with squares in sample A5 are related to the support tape. **b** XRD patterns of samples A1, A2, A4, A3 and A6 recorded employing monochromatised $\text{CuK}\alpha$ radiation (1.54 Å)

characteristic of the SO_4 bending mode, and the oscillation of the free and bound $(\text{SO}_4)^{2-}$ ion respectively [48, 49]. The Raman spectra from the samples investigated also indicated bands related to cadmium sulfide and its multi-phonon resonant scattering. More specifically, the bands at 238, 305, and 633 cm^{-1} are ascribed to the transverse optical (TO) and longitudinal optical (LO and 2LO) modes of cadmium sulfide respectively, while the bands at 218 and 346 cm^{-1} are ascribed to the multi-phonon modes [50, 51]. Previous studies have suggested that the increase of zinc content in the $\text{Cd}_{1-x}\text{Zn}_x\text{S}$ solid solutions is likely to be associated with the disappearance of the multi-phonon modes and the shift of the LO mode band to lower wavenumbers [46]. The presence of bands related to the multi-phonon modes in the Raman spectra from the samples investigated might be due to the presence of only a small proportion of zinc in the $\text{Cd}_{1-x}\text{Zn}_x\text{S}$ solid solution, as suggested by elemental analysis. Bands related to a drying oil present as binding medium were detected at 869, 1063 and 1080 cm^{-1} and, in sample A5, which was examined in the range 180 to 3000 cm^{-1} , additional bands for oil at 1304, 1441, 1657, 1740, 2853, and 2909 cm^{-1} could also be detected [52].

The distribution of sulfides/sulfates in the paint cross-section was achieved through SR μXRF chemical state maps of samples A4, A7, A9 and A12 (Fig. 4 and Additional file 1: Fig. S8). In the bulk of all the samples sulfides were detected, which can be associated to the preserved pigment ($\text{Cd}_{1-x}\text{Zn}_x\text{S}$). In the samples A7, A9 and A12, a layer of sulfates was found on the surface, while in sample A4 sulfides have been mainly detected in the whole paint layer, with a localised agglomerate of sulfates that well corresponds to the elemental distribution of Zn. The localisation of sulfates at the paint surface confirms their presence as degradation products of CdS, due to its interaction with the environment [23]. The agglomerates can be instead related to the formation of metal soaps [13].

The organic composition of the paints analysed using GC-MS, showed that all the samples from paintings and studio materials are bound in drying oils. All chromatograms obtained after transesterification of the paint fragments and subsequent GC-MS analysis showed the presence of the typical fatty acids characteristic of siccativ oils: saturated mono-fatty acids, from C8 to C26 (palmitic and stearic being the most abundant); saturated di-fatty acids (azelaic, suberic and sebacic acids in particular), as the most abundant oxidation products;

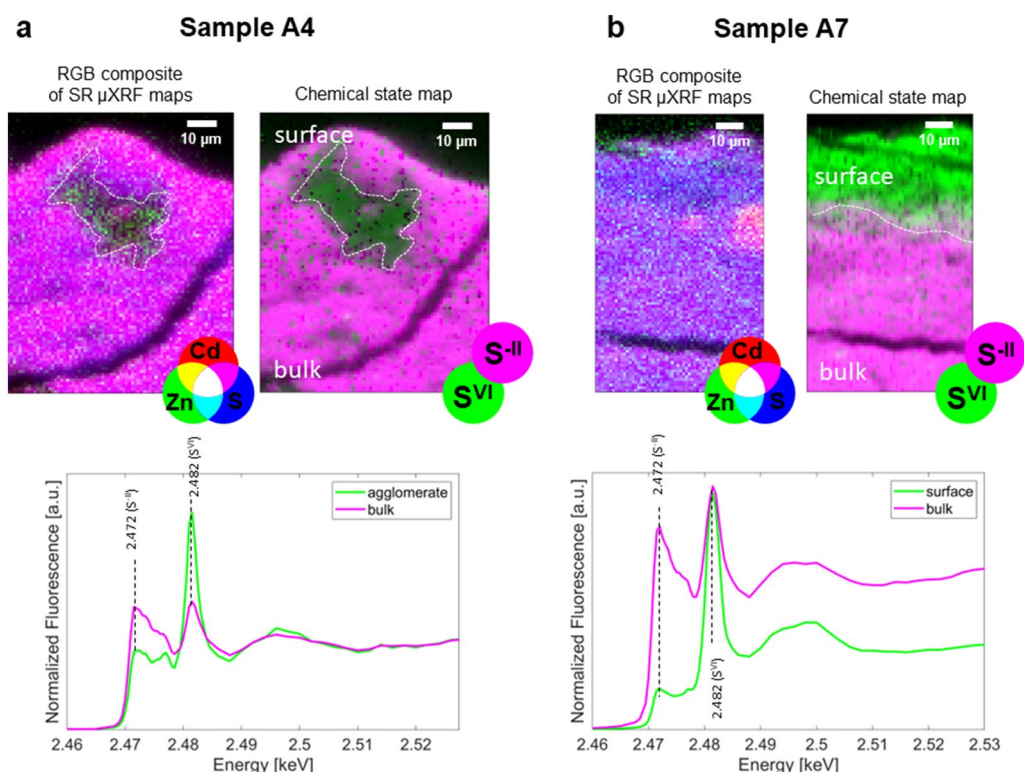


Fig. 4 False colour RGB composite image generated following SR μXRF maps of Cd/Zn/S and $\text{S}^{\text{II}}/\text{S}^{\text{VI}}$ [step size (h × v), $1 \times 1\ \mu\text{m}^2$; exp. time, 10 ms/pixel] and average XANES spectra recorded at the S K-edge of selected ROIs belonging to sample A4 and A7. It is noted that the detection limit for Zn L-lines in the current experimental conditions is very low

unsaturated fatty acids (mainly oleic acid); glycerol (and glycerol derivatives); oxo-, hydroxy- and metoxy- octadecanoic acids as by-oxidation products of unsaturated fatty acids.

Based on the ratios between palmitic to stearic acid (P/S) and the presence/absence of peculiar fatty acids or bio-markers [34, 37, 43], samples from artworks were found to contain different kind of drying oils. Specifically, sample A2 presented the typical chromatographic profile of a cold-pressed linseed oil-based paint, with a P/S=1.87. Sample A7, on the other hand, was characterised by the presence of specific markers related to stand-linseed oil, such as 7-(*o*-pentylphenyl)-heptanoic acid and 9-(*o*-propylphenyl)-nonanoic acid [53]. Safflower oil was likely identified in sample A9 due to the P/S=2.20 and a significant presence of behenic and arachidic acids [39]. This diversity of siccative oils used reflects the complexity of the composition of twentieth century manufactured artists' oil paints, as reported in the specific literature [34, 37, 43, 54]. Similarly, in the samples taken from the artist's oil paint tubes, the presence of a binder consisting of linseed oil was detected in A3 and A6, while safflower or sunflower oil was detected in sample A5. Sample A3 also contain an alkyd-based resin, whose typical components were identified by GC-MS. This could be related to an oil-modified alkyd resin or maybe due to a contamination.

The complexity of the commercial paints analysed was determined also by the detection of several organic additives. For example, in sample A3 traces of beeswax were detected, likely used as a paint stabiliser. In sample A5, a Pinaceae resin (i.e., colophony) was found, probably added as a thickener. Lastly, sample A6 was found to contain metal stearates added as dispersing agents [39].

Linseed oil and a Pinaceae resin were found in the samples taken from the artist's palettes. The resin may

be present as a commercial additive or added by the artist for the purpose of thickening the paint on the palette [34]. Different drying rates were registered, according to the Azelaic to Palmitic (A/P) and Oleic to Stearic (O/S) molar ratios, which may be related to both the different thickness of the samples and their exposure to oxygen [55, 56]. In addition, as is well known, the presence of metal cations can strongly influence the drying of oil paints [57]. It is significant to note that in correspondence with the identification of Zn by elemental analysis, there was also a higher abundance of oleic acid, which can be quantified by the O/S molar ratio, which was already reported in literature as typical of twentieth century Zn-containing white paint [58, 59].

Photoluminescence properties

Under UV illumination, many of the paintings present a bright pink/orange luminescence in the deteriorated CdY areas (Fig. 5). This peculiar and intense emission has been observed also in other paintings with degraded CdY paints [20, 60]. Its origin has been related to surface crystal defects in reactive cadmium yellow paints, possibly manufacturing using nanocrystalline or poorly crystalline CdS pigments [21, 22].

To characterise the luminescent properties of the paints, all samples were analysed with time-gated hyperspectral micro-imaging and results are summarised in Table 2. Paint tube samples containing crystalline CdS (samples A3 and A6) have a sharp nanosecond emission (peaked at 515 and 517 nm, respectively) and a microsecond emission spectrally broad and peaked above 850 nm. These two emission bands are related to the near band edge (NBE) and deep trap states (DTS) emissions of pure CdS, respectively [50, 61]. Instead, poorly crystalline CdY paint tube (sample A5) shows a weak NBE emission peaked at 485 nm, and a broad microsecond emission

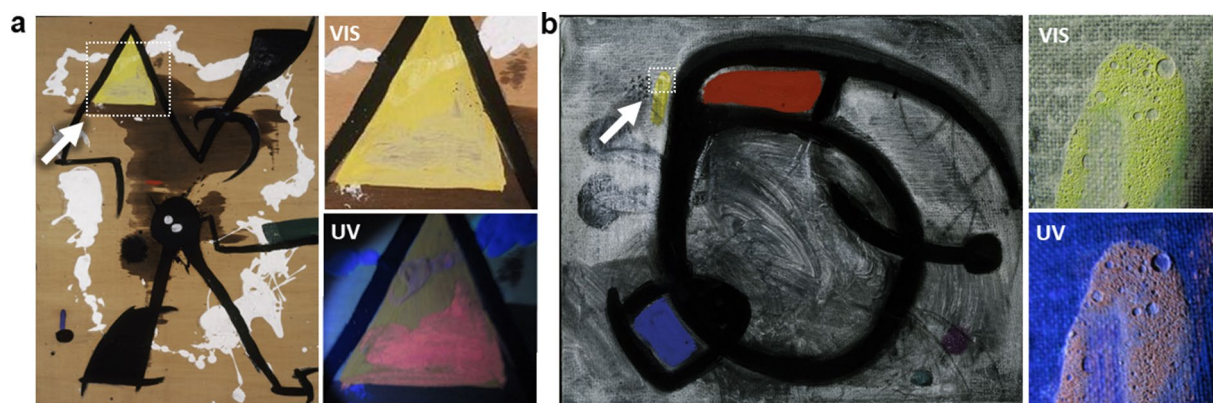


Fig. 5 Deteriorated yellow pigment in artworks *Untitled* (FPJM-00135) (a) and *Untitled* (FPJM-00034) (b) with yellow paints details (white dotted rectangles) under visible light and UV light, showing a peculiar pink/orange luminescence

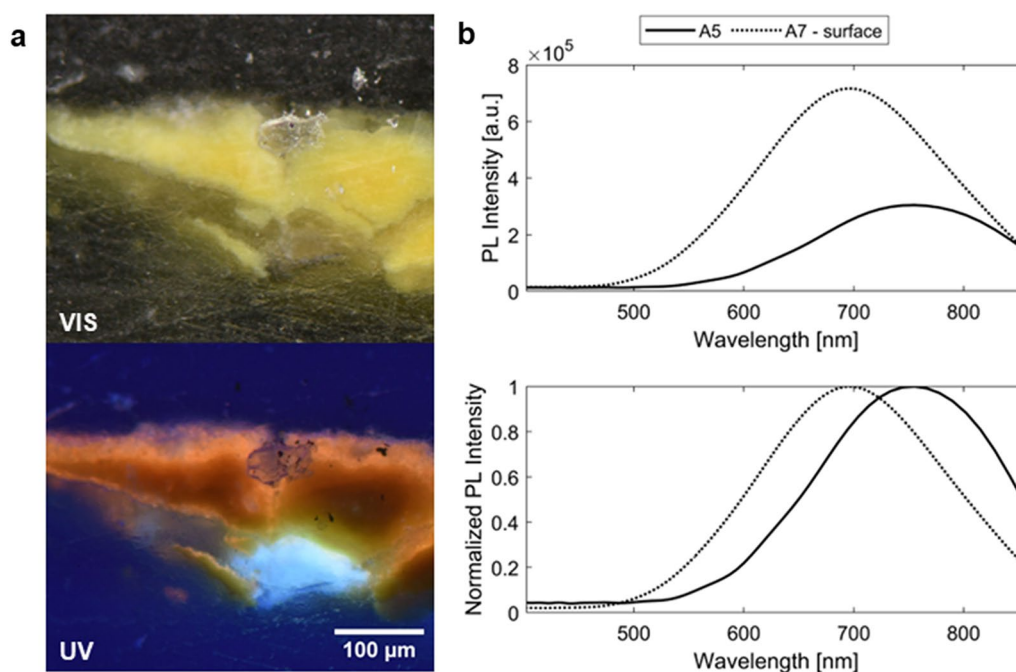


Fig. 6 **a** Cross section of sample A7 under visible and UV light. **b** Time-gated photoluminescence microsecond emission spectra of samples A5 and A7 (surface)

peaked above 750 nm, ascribed to $\text{Cd}_{1-x}\text{Zn}_x\text{S}$ pigment (with $x \sim 0.16$) accordingly to the position of the NBE emission [50, 61].

On their turn, most of the degraded samples from artworks and palettes present an emission, occurring at the microsecond timescale, heterogeneously distributed along the paint stratigraphy (Additional file 1: Fig. S9). Indeed, as illustrated in Fig. 6a for sample A7, the paint surface displays an emission much more intense than the

one from the bulk, suggesting that it is linked to degradation at the paint surface. The strong intensity of the emission at the sample surface, which optically diffuses in the surrounding paint layers, prevents a quantitative comparison of the spectral and lifetime behaviour from the innermost parts of the paint. Despite this, it is worth noting that the emission at the paint surface, peaked at around 650–700 nm, occurs at shorter wavelengths than the emission observed in the poorly crystalline tube

Table 3 Interpretation of the results achieved through the multi-analytical characterisation performed on the samples

Sample name	Interpretation
Artworks	A2 Poorly crystalline $\text{Cd}_{1-x}\text{Zn}_x\text{S}$ ($x \ll 1$), oil binder, degradation products/compounds due to oil/pigment interaction/additives: sulfates, carboxylates, oxalates
	A7 Poorly crystalline $\text{Cd}_{1-x}\text{Zn}_x\text{S}$ ($x \ll 1$), oil binder, degradation products/compounds due to oil/pigment interaction/additives: sulfates, carboxylates
	A9 Poorly crystalline CdS, oil binder, degradation products: sulfates
Oil paint tubes	A3 Crystalline CdS, oil binder, magnesium carbonate additive
	A5 Poorly crystalline $\text{Cd}_{1-x}\text{Zn}_x\text{S}$ ($x \ll 1$), oil binder, degradation products/compounds due to oil/pigment interaction/additives: sulfates, carboxylates
	A6 Crystalline CdS, oil binder, magnesium carbonate additive, compounds due to oil/pigment interaction: oxalates
Artist palettes	A1 Poorly crystalline $\text{Cd}_{1-x}\text{Zn}_x\text{S}$ ($x \ll 1$), oil binder, degradation products/compounds due to oil/pigment interaction/additives: sulfates, carboxylates, oxalates
	A4 Poorly crystalline $\text{Cd}_{1-x}\text{Zn}_x\text{S}$ ($x \ll 1$), oil binder, degradation products/compounds due to oil/pigment interaction/additives: sulfates, carboxylates
	A12 Poorly crystalline $\text{Cd}_{1-x}\text{Zn}_x\text{S}$ ($x \ll 1$), oil binder, degradation products/compounds due to oil/pigment interaction/additives: sulfates, carboxylates, oxalates

sample A5 (Fig. 6b). Indeed, the features of this intense microsecond emission resembles the orangish emission observed in other artworks with degraded CdY [21] and can be ascribed to DTS emission of cadmium-based paints with a high density of crystal defects. It is worth noting that, due to the absence of NBE emission, it was not possible to exactly establish the possible Zn content on the basis of the NBE shift [50]. Nonetheless, the low percentage of Zn detected through elemental analysis does not account for the shift observed in the trap state emission.

Summary of the multi-analytical characterisation

The multi-analytical approach adopted here has allowed us to provide an interpretation of each samples analysed, summarised in Table 3. Samples from artworks, palettes and from the paint tube by *Lefebvre-Foinet* are made of poorly crystalline $\text{Cd}_{1-x}\text{Zn}_x\text{S}$, with a low percentage of zinc, as demonstrated by the combined results from elemental analysis, XRD and Raman. The presence of Zn has been associated with the cadmium pigment in solid solution $\text{Cd}_{1-x}\text{Zn}_x\text{S}$, rather than to the widely diffused white pigment zinc white (ZnO), since this compound was not detected by any of the techniques used. Contrastingly, *Mir* brand paints (samples A3 and A6), were found to be composed of crystalline CdS paint with the presence of MgCO_3 as an extender (as highlighted by EDX analysis and FTIR).

All pigments are dispersed in an oleic matrix (FTIR, Raman and GC–MS) with different kind of organic additives (GC–MS). Samples from artworks, palettes and from the paint tube by *Lefebvre-Foinet* also contain degradation products and compounds due to oil/pigment interaction as cadmium sulfate hydrate (FTIR, SR μXRD and Raman), carboxylates and oxalates (FTIR), while samples A3 and A6 show only the presence of additives such as magnesium carbonate (FTIR, EDX) and small presence of oxalates (sample A6).

Discussion

Based on similarity in chemical composition and the crystalline structure, it is reasonable to assume that Miró used *Lefebvre-Foinet* paint tubes in the artworks that have deteriorated. Until now, it had been assumed that the deterioration was caused by Miró's use of a cheap or poor-quality yellow paints [62]. However, *Lucien Lefebvre-Foinet* was a Parisian manufacture of high-quality paints used by many renowned artists, including Jean Paul Riopelle, Piet Mondrian, Henri Matisse and Alberto Giacometti [63]. More than a hundred oil tubes from this brand are conserved in Miró's studios, five of which are of Cadmium Yellow Lemon No.1, suggesting that this was one of Miró's favourite brands. The low crystallinity

of the pigment may be related to the method used in its synthesis [24], which has enhanced the reactivity of the resulting paints. However, no information is available on the synthesis methods used by the manufacturer. An inscription on some of the boxes containing the paints suggests that they could have been purchased in 1966. To date, the degradation of CdY paint has always been related to the use of imperfect pigments synthesised during the early production period of CdY (between the middle of the nineteenth century and the beginning of the twentieth century) [11, 13, 15]. Pigment produced after this period and after issuing the $\text{Cd}_{1-x}\text{Zn}_x\text{S}$ patent were considered more stable. This research instead clearly shows that reactive pigments were also produced in later times.

In the early twentieth century, $\text{Cd}_{1-x}\text{Zn}_x\text{S}$ -containing paints were manufactured to obtain lighter cadmium yellow shades. The presence of zinc in CdY paints of artworks and palettes may have further influenced the stability of the paint. In fact, previous studies have shown that the stability of the alteration products of CdY paints depends on the Cd/Zn stoichiometry [23], demonstrating that artificially aged $\text{Cd}_{1-x}\text{Zn}_x\text{S}$ samples degrade more than samples composed of CdS, when aged in the same environmental conditions. However, it has also been shown that the only presence of zinc due to the use of $\text{Cd}_{1-x}\text{Zn}_x\text{S}$ does not induce the paint degradation, since the ageing conditions strongly influence CdY paint stability (especially light and high levels of relative humidity [23]). Therefore, it is reasonable to suggest that the presence of zinc, the poorly crystalline (hence reactive) pigment and the environmental conditions may have all contributed to the degradation of CdY paints.

The strong influence of environmental conditions in promoting the degradation of cadmium yellow paints is demonstrated by comparing the two palettes studied. The yellow in one of the palettes (sample A4) is still vibrant and non-degraded, while the yellow in the second palette (sample A12) is visibly degraded, presenting powdery paint and significant discolouration of the vibrant yellow. Despite this, the chemical characterisation of samples from the two palettes showed that they have similar chemical and crystalline properties. Both paints contain poorly crystalline $\text{Cd}_{1-x}\text{Zn}_x\text{S}$ together with carboxylates and sulfates, the latter less abundant in A4 sample and mainly concentrated in the area with Zn. The two palettes were kept in different environmental conditions: a factor that has strongly influenced the relative stability of the paint in each case. The palette containing the vibrant yellow paint was kept inside a display case with no direct sunlight from 1986 until 2018, when it was returned to the studio *Taller Sert*. Therefore, it was protected by the display case for 32 years, and not exposed

to the more extreme fluctuations of relative humidity and intense light levels in the *Taller Sert* to which the second palette was exposed. These findings are in line with the conclusions of the study by Monico et al. [23] in which they state that the photooxidation of cadmium sulfide to cadmium sulfate is triggered by light and high levels of relative humidity; however, it should be noted that traces of hydrated cadmium sulfate were also detected in samples A4 and A5. This compound is known to have been used in the wet synthesis process of CdY and its presence in non-degraded paints may be due to unreacted starting reagents [11, 16].

Poorly crystalline samples showed weak luminescence emission from the layer beneath the surface in CdS samples, while the degraded surface of the same samples presented an intense emission, different from the typical emission of CdS. Based on paint composition (mainly CdS and $3\text{CdSO}_4 \cdot 8\text{H}_2\text{O}$), the emission can be ascribed to a high density of surface defects in the degraded poorly crystalline CdS, rather than to other emitting components. Moreover, the comparison between less degraded samples (sample A4) and the sample from a paint tube containing poorly crystalline CdS (sample A5) suggests that the emission properties of CdS-based paints are affected by degradation and that the presence of the intense and peculiar orangish emission in cadmium yellow paints indicates paint degradation.

Conclusions and future perspectives

In this study, the results of analytical characterisation of CdY paint samples from artworks by Joan Miró and from oil paint tubes and palettes kept in his studios has provided evidence of the degradation of CdY paints in his paintings from the 1970s. This expands on earlier research into CdY alteration found in works from 1880 to 1920 [11, 13, 15]. The study has shown that the main compounds formed due to degradation are cadmium sulfates and zinc/cadmium oxalates and carboxylates. The analyses identified the pigment as poorly crystalline $\text{Cd}_{1-x}\text{Zn}_x\text{S}$ with low percentage of Zn. Although the cause of the chemical change leading to deterioration are difficult to assess due to the presence of multiple factors, we hypothesise that the degradation can be related either to (i) the poorly crystalline structure of the pigment—possibly as a result of the manufacturing method, (ii) the presence of zinc, and (iii) the environmental conditions to which artworks have been exposed (intense natural light and RH levels likely to reach 95%). The comparison of the degradation of the paint from palettes stored and displayed under different conditions strongly suggests that the environmental conditions are a major factor contributing to the deterioration of cadmium yellow paint.

This study has implications for the conservation of artworks by Miró and other artists with similar problems of degradation of CdY paints. It is essential that the artworks are stored and exhibited under conditions with controlled light and relative humidity. Cadmium sulfates, the deterioration products that are concentrated on the paint surface, are soluble, so any surface cleaning intervention can lead to their removal. Regarding the application of protective coatings, varnishes or consolidants, more research is required to determine if they are beneficial or detrimental. In a work by Van Gogh, the application of a varnish over early deteriorating yellow paint has resulted in the formation of a brown layer of cadmium oxalates between the paint and the varnish [14]. Methylcellulose has been applied as a consolidant and to enhance the colour in some of Miró's works at the Fundació with satisfactory results, therefore its effectiveness as a consolidant for degraded yellows could be studied and compared to other matte consolidants. Since most of Miro's late works are unvarnished, glazing with UV-filtering glass can also be an effective solution to protect artworks with fragile and degraded surfaces.

Further research could also include artificially ageing tests (at different ageing steps) on paints prepared from the various paint tubes manufactured by *Lucien Lefebvre-Foinet* kept in the studios. These studies will aim to (i) determine if the paint employed in the artworks and in the paint tubes present the same degradation and under which conditions; (ii) determine the extent of degradation as a function of the ageing time; (iii) establish what can happen with the removal of soluble degradation products as cadmium sulfates and further ageing and assess possible side effect of highly soluble compounds. A program of stepped artificial ageing of paints prepared from *Lucien Lefebvre-Foinet* tube paints (sample A5) could help to verify if the peculiar photoluminescence develops because of degradation, and at which stage of degradation is detectable. If conclusive, this could lead to a possible use as an early diagnostic tool. Comparative analysis of yellow paint in artworks in the collection of the Fundació that have been kept under the same conditions as the one studied, but still present vibrant yellow, would also yield information on the differences in the pigment composition which have resulted in more stable paint.

Supplementary Information

The online version contains supplementary material available at <https://doi.org/10.1186/s40494-023-00987-4>.

Additional file 1. Additional Information. Pictures of the artworks/materials from which the analysed samples were taken (figures S1, S2) and results of the analyses carried out with the different techniques reported in the main manuscript (figures S3–S9).

Acknowledgements

The authors are grateful to the Fundació Pilar i Joan Miró a Mallorca for providing access to the collections and studio materials, to Patricia Juncosa (Head of the Collections Department) for supervising the project and to the Photographic Archive of the Fundació Pilar i Joan Miró for providing the images for publication. All images © Successió Miró, 2023. We are most thankful to Prof. Gemma Turnes, Universitat de les Illes Balears (UIB), for making possible the collaboration with the UIB to undertake the initial analysis. We acknowledge the European Synchrotron Radiation Facility for provision of synchrotron radiation facilities (proposals HG-179 and HG-172) and we would like to thank Dr. Manfred Burghammer for assistance in using beamline ID13 (proposal HG-172, pilot of a BAG project supported by the European Union's Horizon 2020 research and innovation programme under grant agreement No 870313, Streamline). Authors would like to acknowledge Prof. Lucia Toniolo for the assistance in the FTIR μ ATR measurements and Dr. Letizia Monico for the assistance during SR μ XRF/ μ XANES measurements.

Author contributions

MGL led the research project. MGL and EJD designed the research, examined the paintings and collected all samples. CPC and MB carried out the XRD, SEM-EDX and FTIR analysis. MG and DC carried out the FLIM, TG-HSI analysis and interpretation of results. MG, DC and MC carried out SR μ XRF, μ XANES and μ XRD and interpretation of results. SRA, AN and AB carried out Raman analysis and EDX mapping and contributed to data interpretation. FCI carried out the Py-GCMS and GCMS analysis. MG and MGL prepared the manuscript. All authors read and approved the final manuscript.

Funding

This research was part of a larger research project to study Joan Miró's pigments funded by the Pilar Juncosa & Sotheby's Research Award 2020, granted by the Fundació Miró Mallorca.

Availability of data and materials

Data and analysis collected during the study are available from the authors upon reasonable request.

Declarations

Competing interests

The authors declare no competing interests.

Received: 25 February 2023 Accepted: 20 June 2023

Published online: 17 July 2023

References

- Russell JE, Singer BW, Perry JJ, Bacon A. Investigation of the materials found in the studio of Francis Bacon (1909–1992). *Stud Conserv*. 2012;57:195–206.
- Izzo FC, Zanin C, van Keulen H, da Roit C. From pigments to paints: studying original materials from the atelier of the artist Mariano Fortuny y Madrazo. *Int J Conserv Sci*. 2017;8:547–64.
- Caruso F, Mantellato S, Streeton NLW, Frøysaker T. Unveiling Harriet Backer: ICP–OES study for the characterisation of the colour tubes from her original paint box. *Herit Sci*. 2019;7:1–23.
- La Nasa J, Doherty B, Rosi F, Braccini C, Broers FTH, Degano I, et al. An integrated analytical study of crayons from the original art materials collection of the MUNCH museum in Oslo. *Sci Rep*. 2021;11:7152.
- Gil M, Costa M, Cardoso A, Valadas S, Helvaci Y, Bhattacharya S, et al. On the two working palettes of Almada Negreiros at DN building in Lisbon (1939–1940): first analytical approach and insight on the use of Cd based pigments. *Heritage*. 2021;4:4578–95. <https://miromallorca.com/>.
- Rowell M (ed) Joan Miró. *Escritos y conversaciones*. IVAM; 2002.
- Salvadó N, Molera J, Vendrell-Saz M. Nature and origin of black spots found on Miró paintings: a non-invasive study. *Anal Chim Acta*. 2003;479:255–63.
- O'Donoghue E, Johnson AM, Mazurek J, Preusser F, Schilling M, Walton MS. Dictated by media: conservation and technical analysis of a 1938 Joan Miró canvas painting. *Stud Conserv*. 2006;51:62–8.
- Gomez Lobon M, Juncosa Darder E, Palomino Cabello C, Bauza M. Investigación de los pigmentos utilizados por Joan Miró durante su etapa artística en Mallorca. 24^a Jornada de Conservación de Arte Contemporáneo, MNCARS. Madrid; 2023.
- Fiedler I, Bayard MA. Cadmium yellows, oranges and reds. In: Feller RL, editor. *Artists' pigments a handbook of their history and characteristics*. Cambridge: Cambridge University Press; 1986. p. 65–108.
- Levin BDA, Finnefrock AC, Hull AM, Thomas MG, Nguyen KX, Holtz ME, et al. Revealing the nanoparticle composition of Edvard Munch's The Scream, and implications for paint alteration in iconic early 20th century artworks. *arXiv:190901933*. 2019.
- Monico L, Cartechini L, Rosi F, Chieli A, Grazia C, De Meyer S, et al. Probing the chemistry of CdS paints in The Scream by in situ noninvasive spectroscopies and synchrotron radiation x-ray techniques. *Sci Adv*. 2020. <https://doi.org/10.1126/sciadv.aay3514>.
- Van der Snickt G, Janssens K, Dik J, De Nolf W, Vanmeert F, Jaroszewicz J, et al. Combined use of synchrotron radiation based micro-X-ray fluorescence, micro-X-ray diffraction, micro-X-ray absorption near-edge, and micro-Fourier transform infrared spectroscopies for revealing an alternative degradation pathway of the pigment cadmium yellow. *Anal Chem*. 2012;84:10221–8.
- Leone B, Burnstock A, Jones C, Hallebeek P, Boon JJ, Keune K. The deterioration of cadmium sulphide yellow artists' pigments. In: ICOM committee for conservation triennial meeting, 14th, The Hague, Netherlands. 2005. p. 803–13.
- Pouyet E, Cotte M, Fayard B, Salomé M, Meirer F, Mehta A, et al. 2D X-ray and FTIR micro-analysis of the degradation of cadmium yellow pigment in paintings of Henri Matisse. *Appl Phys A*. 2015;121:967–80.
- Mass J, Sedlmair J, Patterson CS, Carson D, Buckley B, Hirschmugl C. SR-FTIR imaging of the altered cadmium sulfide yellow paints in Henri Matisse's *Le Bonheur de vivre* (1905–6)—examination of visually distinct degradation regions. *Analyst*. 2013;138:6032.
- Mass JL, Opila R, Buckley B, Cotte M, Church J, Mehta A. The photodegradation of cadmium yellow paints in Henri Matisse's *Le Bonheur de vivre* (1905–1906). *Appl Phys A*. 2013;111:59–68.
- Voras ZE, DeGhetaldi K, Wiggins MB, Buckley B, Baade B, Mass JL, et al. ToF–SIMS imaging of molecular-level alteration mechanisms in *Le Bonheur de vivre* by Henri Matisse Zachary. *Appl Phys A Mater Sci Process*. 2015;121:1015–30.
- Van der Snickt G, Dik J, Cotte M, Janssens K, Jaroszewicz J, De Nolf W, et al. Characterization of a degraded cadmium yellow (CdS) pigment in an oil painting by means of synchrotron radiation based X-ray techniques. *Anal Chem*. 2009;81:2600–10.
- Comelli D, MacLennan D, Ghirardello M, Phenix A, Schmidt Patterson C, Khanjian H, et al. Degradation of cadmium yellow paint: new evidence from photoluminescence studies of trap states in Picasso's *Femme (Époque des "Demoiselles d'Avignon")*. *Anal Chem*. 2019;91:3421–8.
- Ghirardello M, Gonzalez V, Monico L, Nevin A, MacLennan D, Patterson CS, et al. Application of synchrotron radiation-based micro-analysis on cadmium yellows in Pablo Picasso's *Femme*. *Microsc Microanal*. 2022;28:1–10.
- Monico L, Chieli A, De Meyer S, Cotte M, de Nolf W, Falkenberg G, et al. Role of the relative humidity and the Cd/Zn stoichiometry in the photooxidation process of cadmium yellows (CdS/Cd_{1-x}Zn_xS) in oil paintings. *Chem Eur J*. 2018;24:11584–93. <https://doi.org/10.1002/chem.201801503>.
- Ghirardello M, Otero V, Comelli D, Toniolo L, Dellasega D, Nessi L, et al. An investigation into the synthesis of cadmium sulfide pigments for a better understanding of their reactivity in artworks. *Dyes Pigment*. 2021;186:108998.
- Cotte M, Gonzalez V, Vanmeert F, Monico L, Dejoie C, Burghammer M, et al. The "historical materials BAG": a new facilitated access to synchrotron X-ray diffraction analyses for cultural heritage materials at the European synchrotron radiation facility. *Molecules*. 2022;27:1997.
- Ashtotis G, Deschildre A, Nawaz Z, Wright JP, Karkoulis D, Picca FE, et al. The fast azimuthal integration Python library: PyFAI. *J Appl Crystallogr*. 2015;48:510–9.

27. Cotte M, Fabris T, Agostini G, Motta Meira D, De Viguierie L, Solé VA. Watching kinetic studies as chemical maps using open-source software. *Anal Chem*. 2016;88:6154–60.
28. Cotte M, Pouyet E, Salomé M, Rivard C, Nolf W De, Castillo-Michel H, et al. The ID21 X-ray and infrared microscopy beamline at the ESRF : status and recent applications to artistic materials e. 2017.
29. Cotte M, Dollman K, Fernandez V, Gonzalez V, Vanmeert F, Monaco L, et al. New opportunities offered by the ESRF to the cultural and natural heritage communities. *Synchrotron Radiat News*. 2022;1–7.
30. Ghirardello M, Manzoni C, Girona M, Alberti R, Lenz R, Zöldföldi J, et al. A novel photoluminescence hyperspectral camera for the study of artworks. *EPJ Plus*. 2021;Submitted.
31. Pagnin L, Calvini R, Sterflinger K, Izzo FC. Data fusion approach to simultaneously evaluate the degradation process caused by ozone and humidity on modern paint materials. *Polymers*. 2022;14:1787.
32. Izzo FC, Balliana E, Perra E, Zendri E. Accelerated ageing procedures to assess the stability of an unconventional acrylic-wax polymeric emulsion for contemporary art. *Polymers*. 2020;12:1925.
33. Izzo FC, Carrieri A, Bartolozzi G, van Keulen H, Lorenzon I, Balliana E, et al. Elucidating the composition and the state of conservation of nitrocellulose-based animation cells by means of non-invasive and micro-destructive techniques. *J Cult Herit*. 2019;35:254–62.
34. Caravá S, Roldán García C, Vázquez de Agredos-Pascual ML, Murcia Mascarós S, Izzo FC. Investigation of modern oil paints through a physico-chemical integrated approach. Emblematic cases from Valencia. *Spain Spectrochim Acta A Mol Biomol Spectrosc*. 2020;240:118633.
35. Izzo FC, Källbom A, Nevin A. Multi-analytical assessment of bodied drying oil varnishes and their use as binders in armour paints. *Heritage*. 2021;4:3402–20.
36. Fuster-López L, Izzo FC, Damato V, Yusà-Marco DJ, Zendri E. An insight into the mechanical properties of selected commercial oil and alkyl paint films containing cobalt blue. *J Cult Herit*. 2019;35:225–34.
37. Fuster-López L, Izzo FC, Andersen CK, Murray A, Vila A, Picollo M, et al. Picasso's 1917 paint materials and their influence on the condition of four paintings. *SN Appl Sci*. 2020;2:2159.
38. Huckle WG, Swiger GF, Wiberley SE. Cadmium pigments: structure and composition. *Ind Eng Chem Prod Res Dev*. 1966;5:362–6.
39. De Viguierie L, Payard PA, Portero E, Walter P, Cotte M. The drying of linseed oil investigated by Fourier transform infrared spectroscopy: historical recipes and influence of lead compounds. *Prog Org Coat*. 2016;93:46–60.
40. Otero V, Sanches D, Montagner C, Vilarigues M, Carlyle L, Lopes JA, et al. Characterisation of metal carboxylates by Raman and infrared spectroscopy in works of art. *J Raman Spectrosc*. 2014;45:1197–206.
41. Hermans JJ, Keune K, Van Loon A, Iedema PD. An infrared spectroscopic study of the nature of zinc carboxylates in oil paintings. *J Anal At Spectrom*. 2015;30:1600–8.
42. Izzo FC, Ferriani B, Van den Berg KJ, Van Keulen H, Zendri E. 20th century artists' oil paints: the case of the Ollii by Lucio Fontana. *J Cult Herit*. 2014;15:557–63.
43. Izzo FC, Van Den BKJ, Van KH, Ferriani B, Zendri E. Modern oil paints—formulations, organic additives and degradation: some case studies. In: Van den Berg KJ, Burnstock A, De Keijzer M, Krueger J, Learner T, De Tagle A, Heydenreich G, editors. *Issues in contemporary oil paint*. Geneva: Springer International Publishing Switzerland; 2014. p. 75–104.
44. Silvester G, Burnstock A, Megens L, Learner T, Chiari G, Van Den Berg KJ. A cause of water-sensitivity in modern oil paint films: the formation of magnesium sulphate. *Stud Conserv*. 2014;59:38–51.
45. Harrison J, Lee J, Ormsby B, Payne DJ. The influence of light and relative humidity on the formation of epsomite in cadmium yellow and French ultramarine modern oil paints. *Herit Sci*. 2021;9:1–17.
46. Simonsen KP, Poulsen JN, Vanmeert F, Ryhl-Svendsen M, Bendix J, Sanyova J, et al. Formation of zinc oxalate from zinc white in various oil binding media: the influence of atmospheric carbon dioxide by reaction with ¹³CO₂. *Herit Sci*. 2020;8:1–11.
47. Otero V, Vilarigues M, Carlyle L, Cotte M, De Nolf W, Melo MJ. A: little key to oxalate formation in oil paints: protective patina or chemical reactor? *Photochem Photobiol Sci*. 2018;17:266–70.
48. Krishnan TS, Narayanan PS. Raman spectrum of crystalline cadmium sulphate. *Proc Indian Acad Sci Sect A*. 1955;41:121–4.
49. Rajadurai G, Raj AP, Pari S, Appl A, Res S. Growth and characterization of cadmium sulphate single crystal by gel growth. *Arch Appl Sci Res*. 2013;5:247–53.
50. Rosi F, Grazia C, Gabrieli F, Romani A, Paolantoni M, Vivani R, et al. UV-Vis-NIR and micro Raman spectroscopies for the non destructive identification of Cd_{1-x}Zn_xS solid solutions in cadmium yellow pigments. *Microchem J*. 2016;124:856–67.
51. Chi TTK, Gouadec G, Colomban P, Wang G, Mazerolles L, Liem NQ. Off-resonance Raman analysis of wurtzite CdS ground to the nanoscale: Structural and size-related effects. *J Raman Spectrosc*. 2011;42:1007–15.
52. Vandenaabeele P, Wehling B, Moens L, Edwards H, De Reu M, Van Hooydonk G. Analysis with micro-Raman spectroscopy of natural organic binding media and varnishes used in art. *Anal Chim Acta*. 2000;407:261–74.
53. van den Berg JDJ. *Analytical chemical studies on traditional oil paints*. Amsterdam: University of Amsterdam; 2002.
54. Fuster-López L, Izzo FC, Piovesan M, Yusà-Marco DJ, Sperti L, Zendri E. Study of the chemical composition and the mechanical behaviour of 20th century commercial artists' oil paints containing manganese-based pigments. *Microchem J*. 2016;124:962–73.
55. Rasti F, Scott G. The effects of some common pigments on the photo-oxidation of linseed oil-based paint media. *Stud Conserv*. 1980;25:145–56.
56. Wexler H. Polymerization of drying oils. *Chem Rev*. 1964;64:591–611.
57. Bonaduce I, Duce C, Lluveras-Tenorio A, Lee J, Ormsby B, Burnstock A, et al. Conservation issues of modern oil paintings: a molecular model on paint curing. *Acc Chem Res*. 2019;52:3397–406.
58. Osmond G. Zinc white: a review of zinc oxide pigment properties and implications for stability in oil-based paintings. *AICCM Bull*. 2012;33:20–9.
59. Jacobsen AE, Gardner WH. Zinc soaps in paints. *Zinc Oleates Ind Eng Chem*. 1941;33:1254–6.
60. Nevin A, Doherty T. The noninvasive analysis of painted surfaces: scientific impact and conservation practice. In: Nevin A, Doherty T, editors. *Smithsonian contributions to museum conservation*. 2016:viii–81.
61. Cesaratto A, D'Andrea C, Nevin A, Valentini G, Tassone F, Alberti R, et al. Analysis of cadmium-based pigments with time-resolved photoluminescence. *Anal Methods*. 2014;6:130–8.
62. Fernández-Villa S, Juncosa Darder E. *Materiales y técnicas pictóricas de Joan Miró. Problemática de conservación*. VII Reunión de Arte Contemporáneo Grupo Español del International Institute of Conservation. Museo Nacional Centro de Arte Reina Sofía; 2006. p. 15–22.
63. Corbeil M-C, Helwig K, Poulin J. *Jean Paul Riopelle: The Artist's Materials*. 2011

Publisher's Note

Springer Nature remains neutral with regard to jurisdictional claims in published maps and institutional affiliations.

Submit your manuscript to a SpringerOpen® journal and benefit from:

- Convenient online submission
- Rigorous peer review
- Open access: articles freely available online
- High visibility within the field
- Retaining the copyright to your article

Submit your next manuscript at ► [springeropen.com](https://www.springeropen.com)

Terms and Conditions

Springer Nature journal content, brought to you courtesy of Springer Nature Customer Service Center GmbH (“Springer Nature”).

Springer Nature supports a reasonable amount of sharing of research papers by authors, subscribers and authorised users (“Users”), for small-scale personal, non-commercial use provided that all copyright, trade and service marks and other proprietary notices are maintained. By accessing, sharing, receiving or otherwise using the Springer Nature journal content you agree to these terms of use (“Terms”). For these purposes, Springer Nature considers academic use (by researchers and students) to be non-commercial.

These Terms are supplementary and will apply in addition to any applicable website terms and conditions, a relevant site licence or a personal subscription. These Terms will prevail over any conflict or ambiguity with regards to the relevant terms, a site licence or a personal subscription (to the extent of the conflict or ambiguity only). For Creative Commons-licensed articles, the terms of the Creative Commons license used will apply.

We collect and use personal data to provide access to the Springer Nature journal content. We may also use these personal data internally within ResearchGate and Springer Nature and as agreed share it, in an anonymised way, for purposes of tracking, analysis and reporting. We will not otherwise disclose your personal data outside the ResearchGate or the Springer Nature group of companies unless we have your permission as detailed in the Privacy Policy.

While Users may use the Springer Nature journal content for small scale, personal non-commercial use, it is important to note that Users may not:

1. use such content for the purpose of providing other users with access on a regular or large scale basis or as a means to circumvent access control;
2. use such content where to do so would be considered a criminal or statutory offence in any jurisdiction, or gives rise to civil liability, or is otherwise unlawful;
3. falsely or misleadingly imply or suggest endorsement, approval, sponsorship, or association unless explicitly agreed to by Springer Nature in writing;
4. use bots or other automated methods to access the content or redirect messages
5. override any security feature or exclusionary protocol; or
6. share the content in order to create substitute for Springer Nature products or services or a systematic database of Springer Nature journal content.

In line with the restriction against commercial use, Springer Nature does not permit the creation of a product or service that creates revenue, royalties, rent or income from our content or its inclusion as part of a paid for service or for other commercial gain. Springer Nature journal content cannot be used for inter-library loans and librarians may not upload Springer Nature journal content on a large scale into their, or any other, institutional repository.

These terms of use are reviewed regularly and may be amended at any time. Springer Nature is not obligated to publish any information or content on this website and may remove it or features or functionality at our sole discretion, at any time with or without notice. Springer Nature may revoke this licence to you at any time and remove access to any copies of the Springer Nature journal content which have been saved.

To the fullest extent permitted by law, Springer Nature makes no warranties, representations or guarantees to Users, either express or implied with respect to the Springer nature journal content and all parties disclaim and waive any implied warranties or warranties imposed by law, including merchantability or fitness for any particular purpose.

Please note that these rights do not automatically extend to content, data or other material published by Springer Nature that may be licensed from third parties.

If you would like to use or distribute our Springer Nature journal content to a wider audience or on a regular basis or in any other manner not expressly permitted by these Terms, please contact Springer Nature at

onlineservice@springernature.com